

# Rapid Prototyping for Multiscale (Micro- to Millimeter) Thermoplastic Structures

Takahito Aruga,<sup>1</sup> Takaaki Abe,<sup>1</sup> Ryo Muramatsu,<sup>1</sup>  
Shunya Okamoto,<sup>2</sup> and Yoshiaki Ukita<sup>3\*</sup>

<sup>1</sup>Integrated Graduate School of Medicine, Engineering and Agricultural Sciences, University of Yamanashi,  
4-3-11 Takeda, Kofu, Yamanashi 400-8511, Japan

<sup>2</sup>Department of Mechanical Engineering, Toyohashi University of Technology,  
Toyohashi, Aichi 441-8580, Japan

<sup>3</sup>Graduate Faculty of Interdisciplinary Research, University of Yamanashi,  
4-3-11 Takeda, Kofu, Yamanashi 400-8511, Japan

(Received September 25, 2023; accepted January 18, 2024)

**Keywords:** molding, hot embossing, microchannel, microfluidics

In this paper, we report on the development of a rapid prototyping technique for thermoplastic microstructures. In particular, this technology is unique in that it has realized a process that can simultaneously form structures ranging from several tens of micrometers to several millimeters in size, which is often required for microfluidic devices. The key technologies in achieving this are the creation of millimeter-scale mold masters by our original wax reflow process and the creation of hot-embossed molds by a two-step casting process. As a result of prototyping, the molding of microfluidic structures with widths ranging from 50 to 500  $\mu\text{m}$  and reagent reservoir shapes with sizes of several millimeters have been realized. In this process, double casting is a special part of this method of realizing multiscale molds. This effect caused some accuracy degradation due to swelling when casting polydimethylsiloxane (PDMS) daughter molds from PDMS mother molds. This effect was only a 3–9 % decrease in the channel cross-sectional area relative to the mold master, as determined by quantitative evaluation. As described above, the proposed process is a promising technology for the rapid prototyping of thermoplastic products, and is required in the research and development of microfluidic devices at a stage close to practical application.

## 1. Introduction

In microfluidics, soft lithography using polydimethylsiloxane (PDMS) as a fundamental material has contributed to the development of microfluidics as a rapid prototyping technique for easily creating highly transparent microfluidic chips with high accuracy.<sup>(1)</sup> It is a photolithographic transfer technique that uses the microstructure of thick-film photoresist as a template to form microfluidic chips with microstructures by transferring the template shape onto highly flexible PDMS. Another feature is that PDMS is flexible and easy to release, allowing

---

\*Corresponding author: e-mail: yukita@yamanashi.ac.jp  
<https://doi.org/10.18494/SAM4667>

microfluidic chips to be formed without damaging the microstructure of the mold formed by the photoresist. This simplicity has made it possible for chemists and biochemists without specialized equipment or knowledge of processing to create their own custom-made microchips for research. Furthermore, the transparency of PDMS is useful for flow observation and fluorescence detection, which has led to the rapid growth of the field of microfluidics (or  $\mu$ TAS, Lab on a chip).

On the other hand, even though PDMS is the gold standard material for the rapid prototyping of microfluidic devices, more material variations are required in terms of mechanical and physicochemical properties to realize practical microfluidic devices.<sup>(2)</sup> Although inorganic materials such as silicon and glass, for which microfabrication techniques have been established in the field of MEMS, could be an option, plastic is the most attractive material from an industrial perspective in terms of cost and productivity, and many attempts to produce plastic microfluidic devices have been reported.<sup>(3)</sup> Injection molding<sup>(4)</sup> and hot embossing<sup>(5)</sup> are common examples of plastic molding, but are not as accessible as soft lithography from a facilities perspective.

On the other hand, a rapid prototyping method for plastics that utilizes PDMS as a template has been developed.<sup>(6–8)</sup> For example, Goral *et al.* achieved rapid prototyping with PDMS molds fabricated by soft lithography and hot embossing with binder clips.<sup>(9)</sup> Thus, this technology is an extremely accessible method.

On the other hand, it is often necessary to simultaneously process millimeter-scale structures along with microfluidic channels in order to increase the volume of containers to store reagents for chemical processes or to increase the volume of reaction products.<sup>(10,11)</sup> Particularly in centrifugal microfluidic channels, such structures are frequently utilized for the purpose of metering reagent volumes<sup>(12)</sup> and adjusting timers.<sup>(13)</sup> We have developed a resin reflow process that can easily and precisely realize such relatively large structures on the scale of several hundred micrometers to several millimeters.<sup>(14,15)</sup> This enables a PDMS device with a multiscale structure that has a microfluidic channel structure and a reagent storage chamber of a scale of a few millimeters. Since PDMS molds with high-precision multiscale structures can be easily realized by using this technology, we have worked to realize the rapid prototyping of plastic products with multiscale structures using this technology. This paper is focused on the accuracy and application limits of the plastic structures realized by this attempt. In particular, the mold manufacturing process requires double casting because of the necessity of the resin reflow process. The effect of these peculiarities on process characteristics will also be reported.

## 2. Materials and Methods

### 2.1 Design of molds

Figure 1 shows a drawing of the photomask used to fabricate the molds. Our initial interest was the effect of the existence of multiscale structures on transferability. To investigate this, four types of mold were prepared. Designs 1A and 1B are patterns with sizes of a few millimeters intended to be the reagent chambers often required in microfluidic devices. As described later,

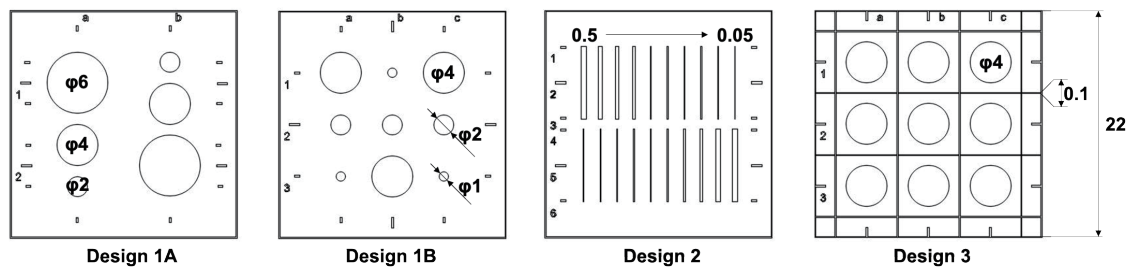


Fig. 1. Designs of molds.

the wax reflow process actually uses this pattern formed with a thick-film photoresist as a footprint to form a hemispherical chamber shape of a few millimeters in size. Design 2 is a typical line-and-space pattern designed for microfluidic channels with a width of 0.05–0.5 mm. Design 3 is intended for molding a more practical microfluidic device-like structure and combines a grid pattern of 0.1-mm-wide microchannels with 4-mm-diameter chambers.

## 2.2 Mold fabrication

The mold master fabrication process is shown in Fig. 2(a). SU8 3050 (KAYAKU Advanced Materials) was applied by spin coating to a silicon wafer (4 inches, As-doped; Frontline Technology) to form a 105- $\mu\text{m}$ -thick resist film. The substrate was irradiated with UV light through the photomask with a pattern shown in Fig. 1, post-baked at 95 °C, and developed with SU8 developer. For Designs 1 and 3, chamber molds were attached by a reflow process. For each pattern, an appropriately sized cylindrical piece of wax (Ferris, File-A-Wax) was placed on the circular SU8 footprint pattern and heated in an oven (AS ONE, EO-300B) at 125 °C for 5 min to melt and reflow the wax. The footprint pattern sizes were 1, 2, 4, and 6 mm diameters., and the wax weights for these were 0.4, 1.7, 12, and 29 mg, respectively. After reflow, the oven was allowed to cool naturally until the inside of the oven reached room temperature, and this was used as the mold master.

Next, the fabrication of the PDMS mold is shown in Fig. 2(b). PDMS (Toray Dow Corning, Silpot 184) is applied to the mold master to a thickness of 2 mm and cured by heating in an oven at 75 °C for 1.5 h. The cured PDMS is peeled from the master, cut into squares of 22 mm side length, and then heated in an oven at 200 °C for 30 min. After treatment with air plasma (SAKIGAKE-Semiconductor Co., Ltd., YHS-R) for 30 s, the films are attached to a glass plate and heated at 75 °C for 15 min on a hot plate for bonding. The PDMS is again treated with air plasma for 30 s and immersed in ultrapure water for 30 min. Then, the mold is dried in a vacuum desiccator for 1 h followed by silanization with 50  $\mu\text{l}$  of trichloro(1H,1H,2H,2H-perfluorooctyl) silane (Sigma-Aldrich, 448931) in a vacuum desiccator for 3 h. Finally, the mother mold is heated in an oven at 120 °C for 30 min. PDMS is applied to the mother mold to a thickness of 3 mm and cured by heating in an oven at 75 °C for 1.5 h. The cured PDMS is peeled off from the mother mold, cut into squares of 29 mm side length, and heated in an oven at 220 °C for 30 min for annealing, to form daughter molds for hot embossing.

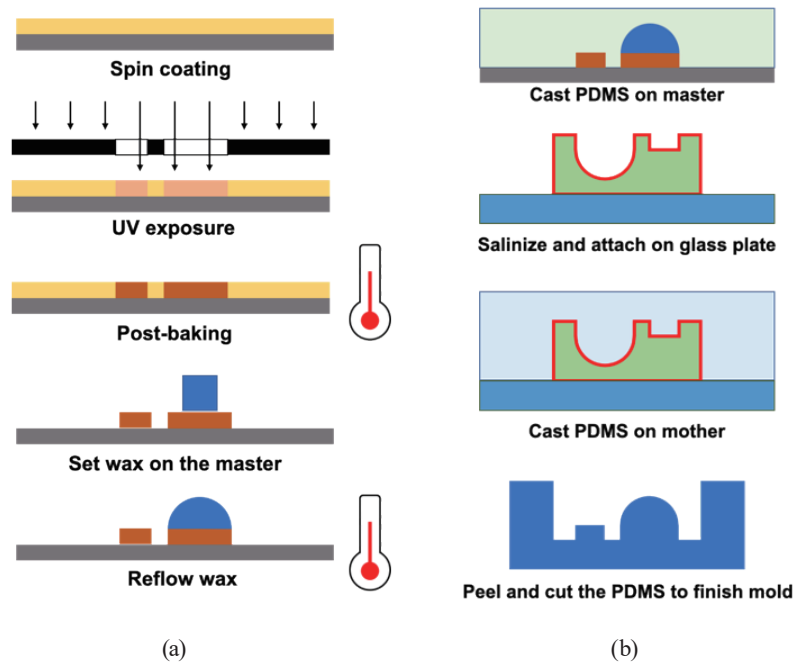


Fig. 2. (Color online) Schematic of molding procedure. (a) Fabrication of mold master and (b) fabrication of mold.

### 2.3 Molding procedure

For hot embossing, the home-made apparatus shown in Fig. 3(a) was used. The prepared hot embossing mold is set in the mold cavity, and 2.25 g of PS pellets (HF77, PS Japan) are set in the mold cavity. The amount of pellets prepared is about 40% more than the final mass of the molded product. In this state, the fixed plate is fixed so that the coils of the heat-resistant spring (Samini, TS162S, spring constant 1.88 N/mm) are in close contact. The initial displacement of the spring is 19.2 mm and the applied pressure is 37.6 N considering the weight of the piston. Therefore, the surface pressure based on the mold area is 90 kPa. The stopper is fixed so that the distance between the plunger surface and the backing plate after molding is 10 mm.

Figure 3(b) shows a schematic of the molding process. As shown in Fig. 3(b), a 0.5-mm-thick silicone spacer is inserted to create a 0.5 mm gap between the surface of the hot embossing mold and the device. This prevents the deformation of the hot embossing mold due to expansion during heating. The hot embossing apparatus setup as described above is installed in an oven (AS ONE, OFP-300V), and molding is performed according to the program of 80 °C for 4 h followed by 155 °C for 10.5 h. The time required to reach each step in heating is set at 30 min, and cooling is accomplished by natural cooling. Since pellets are used in this process instead of preformed plastic plates, the surface pressure gradually decreases as the void space becomes filled with the melting of the pellets. After cooling, the hot embossing equipment is taken out from the oven, the equipment is disassembled, and the molded product is taken out. Finally, excess burrs adhering to the molding are removed using a cutter or other means.

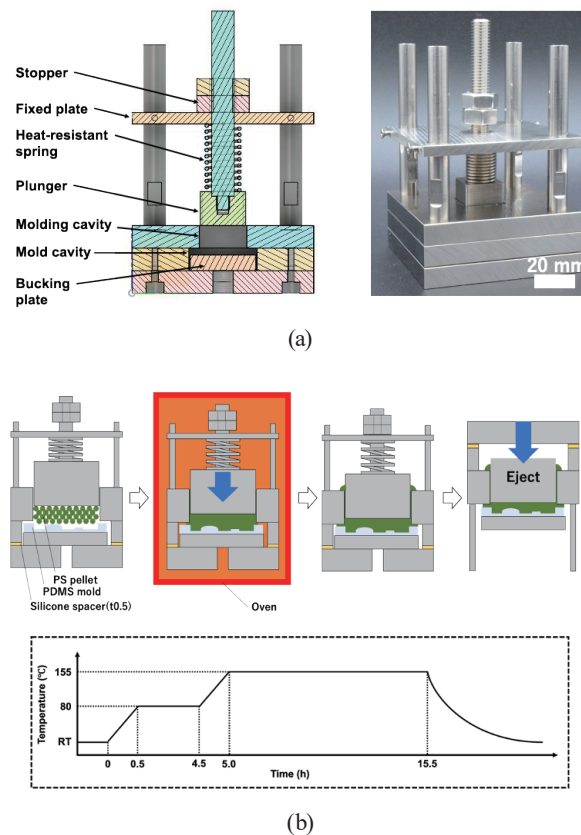


Fig. 3. (Color online) (a) Schematic and photograph of hot embossing apparatus and (b) schematic of molding procedure.

### 3. Results and Discussion

Figure 4 shows a photograph of the appearance of the molded products. Frosted texture and scratches on the surface of the molded product appear because of the transfer of the surface roughness of the molding apparatus. There is no damage to the molded product or mold or bubbles in the bulk that can be seen visually or with a stereomicroscope. In our initial experiments, we used a PDMS mold without annealing at 220 °C. In this case, the surface of the PDMS mold after the experiment was deformed, likely due to contact with the unsoftened plastic pellets. Therefore, this annealing step of the PDMS mold is strongly required to achieve useful products. In addition, since this method takes a longer time than mass production methods such as injection molding, the flow of resin is slower, and the burden on the mold is considered to be relatively small. This is also likely to contribute to reduced damage such as mold deformation.

To investigate detailed processing characteristics, volumetric measurements of the chamber geometry and evaluation of the cross-sectional shape of the microchannel pattern were performed. The Design 1 pattern was utilized to evaluate the molding characteristics of the chambers. The evaluation was performed by comparing the chamber volume of the PS molded product with the volume of the chamber formed by transferring the shape of the master mold onto PDMS. The chamber volume was calculated by filling the chamber with ultrapure water

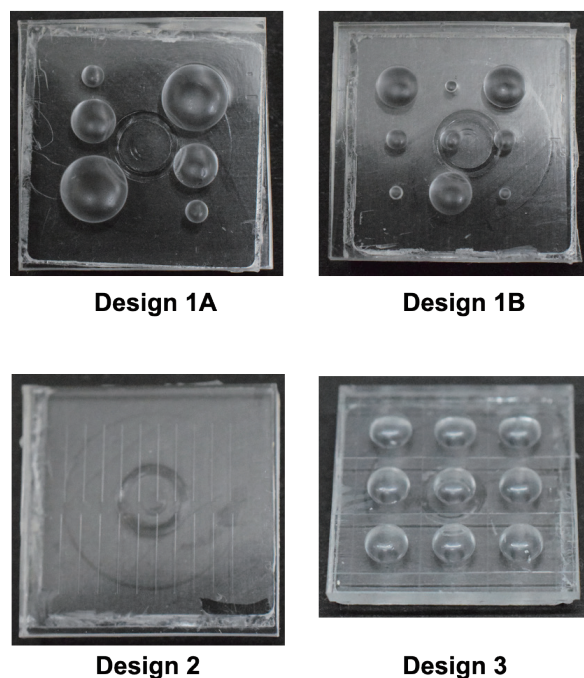


Fig. 4. Photographs of molded products.

and measuring the net water weight with an analytical balance. The results are shown in Fig. 5. No significant volume changes were observed in chambers above  $15 \mu\text{L}$ , indicating that the volume of the master mold was maintained. An increase in error was observed below  $2 \mu\text{L}$ , and this effect resulted in an increase in volume in the  $1 \mu\text{L}$  chamber. We believe that this error is due to the limitation of the volumetric measurement method rather than the accuracy of molding. Specifically, water evaporation during the mass measurement and the adhesion of microscopic bubbles to the PDMS surface may have possible effects.

Patterns of Design 2 were utilized to evaluate the processing characteristics of the microchannel patterns. The cross-sectional shape of the microchannel patterns transferred from the master mold to PDMS and from the PS mold to PDMS were compared and evaluated. Figure 6 shows images of these cross sections taken with a microscope and the results of analyzing these images. An upright pattern was formed even in the pattern with the smallest line width channel fabricated in this study. Because of the low Young's modulus of PDMS, there was concern about pattern buckling during molding, especially in structures with high aspect ratios, when PDMS was used as the mold material. However, this was not the case for structures over  $70 \mu\text{m}$  wide, suggesting that the process is applicable to the fabrication of a typical microfluidic channel. The tilt tended to gradually increase after three repeated processing runs using the same mold. In particular, with respect to the  $50\text{-}\mu\text{m}$ -wide structure, the tilt angle reached up to  $3$  to  $9^\circ$ . Therefore, it was shown that shape control problems arise when the aspect ratio reaches about 2 in terms of the tilt of the microchannel. A decrease of 3–9% was also observed for the cross-sectional area of the microchannel. The cause of this will be discussed later.

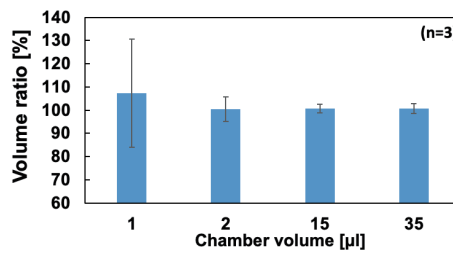


Fig. 5. (Color online) Evaluation of molding characteristics of millimeter-scale chambers based on volume change.

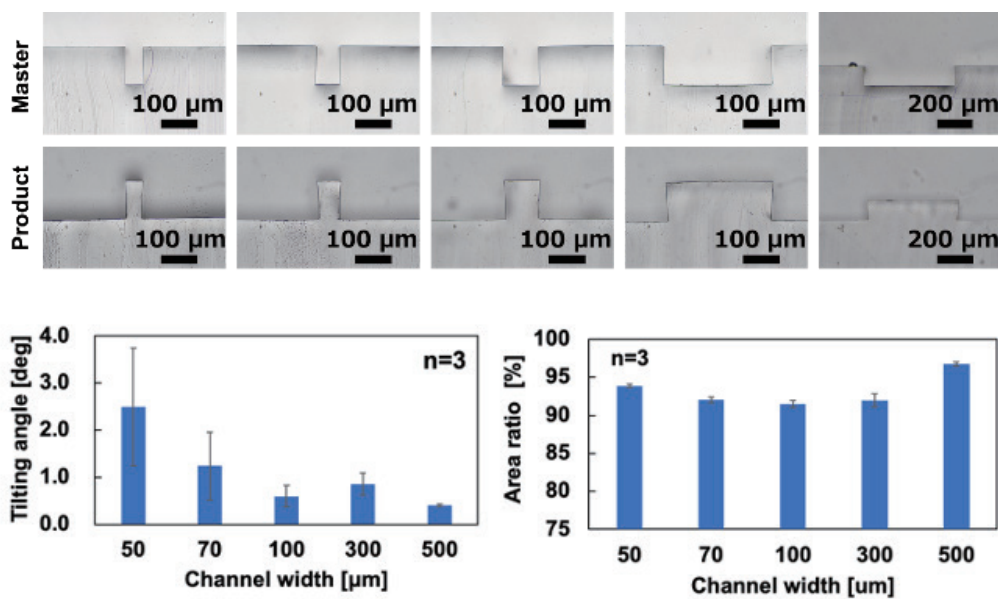


Fig. 6. (Color online) Evaluation of molding characteristics of microchannel structure.

Next, Fig. 7 shows the results of molding with multiple hot embossing molds made repeatedly from the same mother mold. As the number of replications of the hot-embossed mold increases, the decrease in cross-sectional area and the tilt of the channel become more pronounced. From this, we considered that the mother mold swells with each replication of the hot embossing mold. In other words, the PDMS prepolymer diffuses into the mother mold, causing the mold surface to swell and become fatter than before casting, as shown in Fig. 8. Once the prepolymer entrapped in the mother mold forms cross-links, the effect of this swelling becomes irreversible, even after replication. As a result, the daughter mold, which is the inversion of this pattern, becomes skinnier, resulting in a reduced cross-sectional area of the microchannel. To realize multiscale master molds that cannot be processed by photolithography, in our method, a wax reflow process is introduced. Because this reflow process is additive manufacturing, it can only

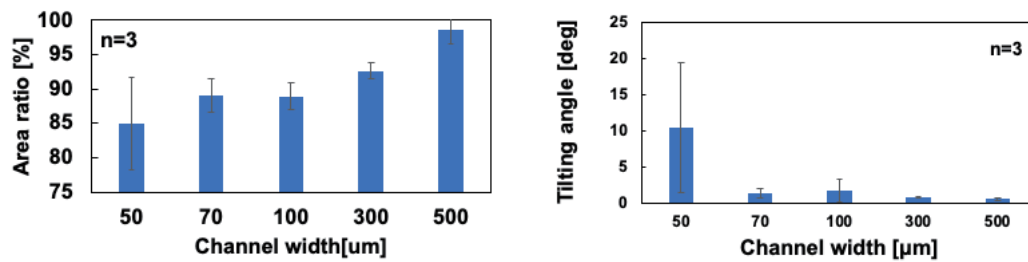


Fig. 7. (Color online) Change in channel molding accuracy when molding molds are repeatedly manufactured from the same master mold.

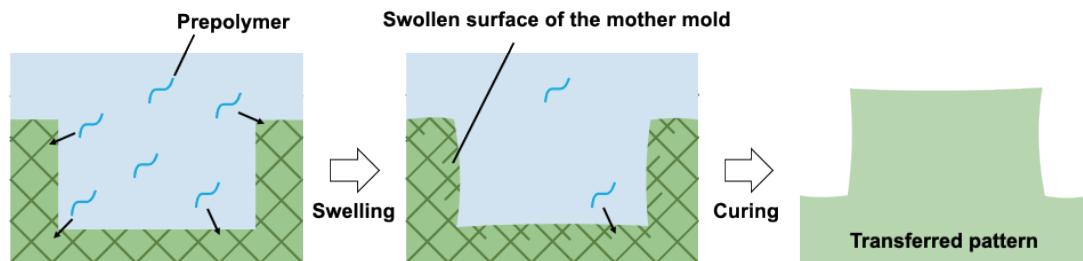


Fig. 8. (Color online) Effect of swelling on the deformation of the mold.

realize master molds with negative geometry of the target structure. Double casting is needed to turn this into a PDMS transfer to obtain a negative mold. The above-described swelling is a trade-off for the adoption of the double-casting process and is a unique problem of this method. As a solution, it is necessary to adopt measures to prevent prepolymer diffusion, such as the formation of an anti-diffusion coating on the PDMS mother surface and pattern replication using different materials such as epoxy resins.

Next, Fig. 9 shows the processing characteristics of a mold with a multiscale structure. Design 3 mold shown in Fig. 9(a) was used for this experiment to evaluate how the chamber volume shown in Fig. 9(b) and the microchannel cross-sectional area shown in Fig. 9(c) were distributed within the pattern. As for the chamber volume, although there was a slight decrease (less than 2%) compared with the master, it can be concluded that the shape was transferred without bias across the entire pattern. In the model of the lattice-shaped channel shown in Fig. 9(c), an increase in the cross-sectional area owing to mold damage, possibly as a result of contamination, was observed at observation position 1, but typically, there was a decrease in the cross-sectional area, possibly due to swelling of the PDMS as described earlier. Although the cross-sectional area tended to decrease slightly at the periphery of the pattern compared with the center of the pattern, the shape of the mold appeared to be faithfully transferred as far as the cross-sectional shape of the microchannel pattern was observed. Therefore, it was difficult to believe that the obstruction of the chamber pattern was the cause of the obstruction of the supply of the resin material. In Design 3, this trend was also somewhat more pronounced when multiple



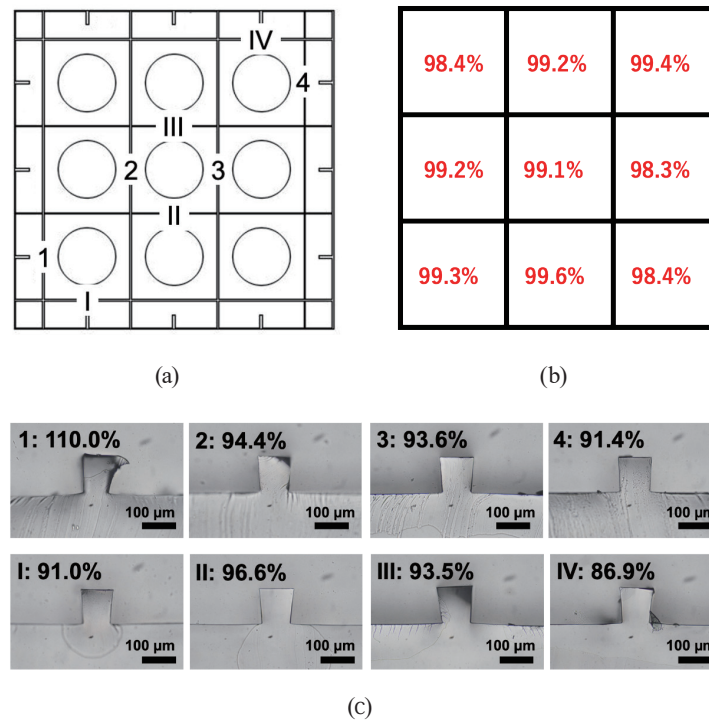


Fig. 9. (Color online) Results of hot embossing with multiscale PDMS mold. (a) Symbols of the observed parts, (b) distribution of volumetric change of the embossed millimeter-scale chambers, and (c) observed cross-sectional images of the microchannel patterns.

daughter molds were processed using the same mother mold. Therefore, we assumed that the swelling of PDMS was also responsible for the reduction in the cross-sectional area described here.

#### 4. Summary

In this study, we developed a hot-embossed mold with multiscale microstructures and realized the rapid prototyping of plastic molded products using this mold. The hot-embossed molds were made by double casting from mold masters that were formed into millimeter-size structures by a wax reflow process. Because of the nature of the double casting process with PDMS, the reduction in microchannel cross-sectional area was likely to be a limitation to some extent, but this could be resolved by utilizing different materials or by applying measures such as anti-diffusion treatment of the prepolymer. Initially, we were concerned that the mixing of structures with different scale orders might cause, for example, partial resin supply shortages. However, we demonstrated that this method can simultaneously form microfluidic channels of typical dimensions and chamber structures of a few millimeters in size, which are useful as reservoirs for reagents.

Plastics have been considered a practical material for microfluidic chips because of their mechanical properties, transparency, and cost. However, the fabrication of microfluidic chips with plastic is usually a hurdle to tackle in research and development due to the financial and

time costs involved in processing the molds. Although the proposed method is limited for mass production, it is possible to fabricate plastic molded products at a low cost and within a few weeks, which is significantly shorter than by conventional molding techniques, even if the product volume is small. This makes it suitable for preliminary studies before fabricating metallic molds for mass production. Moreover, it is a simple process that combines the usual soft lithography with a wax reflow process; therefore, we believe that it is a feasible method for many researchers in the microfluidics community, and we hope that this method will be of help to other researchers.

### Acknowledgments

This work was supported by JKA and its promotion funds from KEIRIN RACE. PS pellets were supplied by MIYAGAWA KASEI INDUSTRY Co., Ltd. We would like to express our gratitude for their support of this research.

### References

- 1 J. C. McDonald, D. C. Duffy, J. R. Anderson, D. T. Chiu, H. Wu, O. J. A. Schueller, and G. M. Whitesides: *Electrophoresis* **21** (2000) 27. [https://doi.org/10.1002/\(SICI\)1522-2683\(20000101\)21:1<27::AID-ELPS27>3.0.CO;2-C](https://doi.org/10.1002/(SICI)1522-2683(20000101)21:1<27::AID-ELPS27>3.0.CO;2-C)
- 2 S. M. Schott and Z. Ali: *Micromachines* **12** (2021) 319. <https://doi.org/10.3390/mi12030319>
- 3 Y. Juang and Y. Chiu: *Polymers* **14** (2022) 2028. <https://doi.org/10.3390/polym14102028>
- 4 J. Giboz, T. Copponnex, and P. Méle: *J. Micromech. Microeng.* **17** (2007) R96. <https://doi.org/10.1088/0960-1317/17/6/R02>
- 5 M. Asif, R. N. Tait, and P. Berini: *Microsystem Technologies* **27** (2021) 3899. <https://doi.org/10.1007/s00542-020-05188-8>
- 6 J. Narasimhan and I. Paputsky: *J. Micromech. Microeng.* **14** (2004) 96. <https://doi.org/10.1088/0960-1317/14/1/013>
- 7 M. Kim, B-U. Moon, and C. H. Hidrovo: *J. Micromech. Microeng.* **23** (2013) 095024. <https://doi.org/10.1088/0960-1317/23/9/095024>
- 8 B.-K. Lee, and B.: *J. Mech. Sci. Technol.* **29** (2015) 5063. <https://doi.org/10.1007/s12206-015-1102-1>
- 9 V. N. Goral, T.-C. Hsieh, O. N. Petzold, R. A. Faris, and P. K. Yuen: 14th Int. Conf. Miniaturized System for Chemistry and Life Sciences (MicroTAS2010) 1214–1216. <https://doi.org/10.1088/0960-1317/21/1/017002>
- 10 D. Natsuhara, R. Saito, H. Aonuma, T. Sakurai, S. Okamoto, M. Nagai, H. Kanuka, and T. Shibata: *Lab Chip* **21** (2021) 4779. <https://doi.org/10.1039/D1LC00829C>
- 11 S. T. Krauss, M. S. Woolf, K. G. Hadley, N. M. Collins, A. Q. Nauman, and J. P. Landers: *Sens. Actuators, B* **284** (2019) 704. <https://doi.org/10.1016/j.snb.2018.12.113>
- 12 S. Lutz, P. Weber, M. Focke, B. Faltin, J. Hoffmann, C. Müller, D. Mark, G. Roth, P. Munday, N. Armes, O. Piepenburg, R. Zengerle, and F. Stetten: *Lab Chip* **10** (2010) 887 <https://doi.org/10.1039/b921140c>
- 13 S. Okamoto, and Y. Ukita: *RSC Adv.* **7** (2017) 35869. <https://doi.org/10.1039/C7RA03721J>
- 14 S. Okamoto, and Y. Ukita: *Micro and Nano Eng.* **8** (2020) 100055. <https://doi.org/10.1016/j.mne.2020.100055>
- 15 T. Abe, S. Okamoto, and Y. Ukita: *Sens. Mater.* **33** (2021) 4441. <https://doi.org/10.18494/SAM.2021.3379>